

Defects in Carbon Nanotubes

J.-C. CHARLIER*

Unit of Physico-Chemistry and Physics of Materials (PCPM),
Research Center on Microscopic and Nanoscopic Materials
and Electronic Devices (CERMIN), Catholic University of
Louvain, Place Croix du Sud 1,
B-1348 Louvain-la-Neuve, Belgium

Received January 23, 2002

ABSTRACT

Carbon nanotubes are quasi one-dimensional nanostructures with unique electrical properties that make them prime candidates for molecular electronics, which is certainly a most promising direction in nanotechnology. Early theoretical works predicted that the electronic properties of “ideal” carbon nanotubes depend on their diameter and chirality. However, carbon nanotubes are probably not as perfect as they were once thought to be. Defects such as pentagons, heptagons, vacancies, or dopant are found to modify drastically the electronic properties of these nanosystems. Irradiation processes can lead to interesting, highly defective nanostructures and also to the coalescence of nanotubes within a rope. The introduction of defects in the carbon network is thus an interesting way to tailor its intrinsic properties, to create new potential nanodevices. The aim of the present Account is to investigate theoretically the effects of different types of defects on the electronic properties of carbon nanotubes, and to propose new potential applications in nanoelectronics.

1. Introduction

Carbon nanotubes are an interesting class of nanostructures which can be thought to arise from the folding of a graphene sheet, which is a planar crystalline structure of hexagonal carbon rings, resembling chicken wire. The nanotubes are usually described using the chiral vector (AA' in Figure 1), $C_h = n \times a_1 + m \times a_2$, which connects two crystallographically equivalent sites (A and A') on a graphene sheet (where a_1 and a_2 are unit vectors of the hexagonal honeycomb lattice and n and m are integers) (see Figure 1). This chiral vector C_h also defines a chiral angle θ , which is the angle between C_h and the zigzag direction of the graphene sheet (Figure 1). Each nanotube topology is usually characterized by these two integer numbers (n,m), thus defining some peculiar symmetries such as *armchair* (n,n) and *zigzag* ($n,0$) classes (see Figure 2).

In 1992, a few theoretical works^{1–3} predicted that the electronic properties of “ideal” carbon nanotubes depend on the width of the graphene sheet (diameter of the tube) and the way it is folded (chirality of the tube), which are both functions of (n,m). The electronic properties of a nanotube vary in a periodic way between being metallic

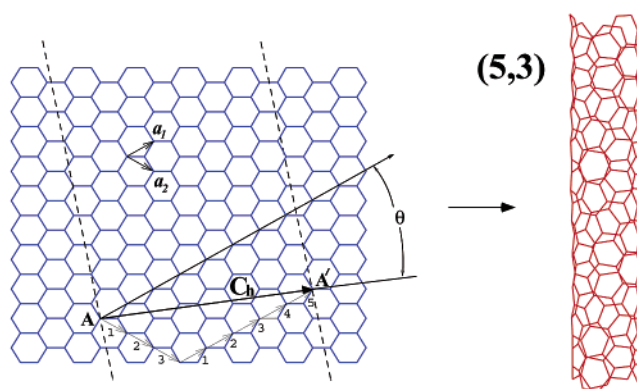


FIGURE 1. Schematic diagram showing the possible wrapping of the two-dimensional graphene sheet into tubular forms. In this example, a (5,3) nanotube is under construction, and the resulting tube is illustrated on the right.

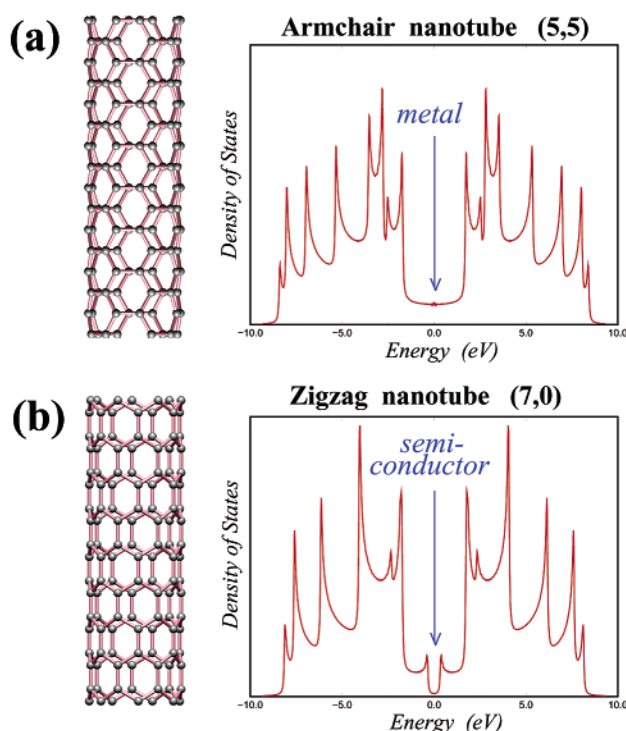


FIGURE 2. Electronic properties of two different carbon nanotubes. (a) The *armchair* (5,5) nanotube exhibits a metallic behavior (finite value of charge carriers in the DOS at the Fermi energy, located at zero). (b) The *zigzag* (7,0) nanotube is a small gap semiconductor (no charge carriers in the DOS at the Fermi energy). Sharp spikes in the DOS are van Hove singularities (a,b).

and semiconductor and follows a general rule: if $(n - m)$ is a multiple of 3, then the tube exhibits a metallic behavior (finite value of carriers in the density of states at the Fermi energy); if $(n - m)$ is not a multiple of 3, then the tube exhibits a semiconducting behavior (no charge carriers in the density of states at the Fermi energy) (see Figure 2).

Five years later, using scanning tunneling microscope probes at low temperature,^{4,5} experimentalists measured

Jean-Christophe Charlier studied physics at the Catholic University of Louvain (UCL-Belgium) in the Faculty of Applied Science for Engineering and got his Ph.D. in 1994. His postdoctoral work was done at EPFL (Lausanne, Switzerland) with Prof. R. Car, where he did pioneering work on the microscopic growth mechanisms for carbon nanotubes using quantum molecular dynamics. His major subjects are solid-state theory, ab initio calculations, and the materials science of carbon. He is a senior research associate of the National Fund for Scientific Research of Belgium and associate professor at the Catholic University of Louvain.

* E-mail: charlier@pcpm.ucl.ac.be.

the electronic structure (density of electronic states, DOS) and physical structure (the nanotube diameter and helicity, which are directly related to (n,m)), confirming the theoretical predictions. Sharp peaks (van Hove singularities) in the DOS, which are the characteristic signature of the strongly one-dimensional nature of the conduction within a 1D system, were also observed and compared to the theoretical models (Figure 2).

The development of nanoelectronics based on nanotubes is certainly a most promising direction in nanotechnology. With these nanocylinders, physicists have found a 1D carbon-based ideal molecule that can conduct electricity at room temperature with essentially no resistance. This phenomenon is known as ballistic transport, where the electrons can be considered as moving freely through the structure, without any scattering from atoms or defects. However, although the nanotube structure is highly perfect, the introduction of defects in the carbon network can lead to interesting properties and new potential nanodevices. The aim of the present Account is to investigate the effects of different defects on the electronic properties of carbon nanotubes. The possible defective structures can be classified into four main groups: *topological* (introduction of ring sizes other than hexagons), *rehybridization* (ability of carbon atom to hybridize between sp^2 and sp^3), and *incomplete bonding defects* (vacancies, dislocations, ...) and *doping* with other elements than carbon.

2. Finite Size and Capping Topologies

Due to their finite size, an interesting structural feature occurs near the ends of all tubes from the closure of the graphene cylinders by the incorporation of topological defects such as pentagons in the hexagonal carbon lattice. The finite aspect of carbon nanotubes imposes their electronic properties to be affected, although only fairly locally, by the tip structure. In view of the large aspect ratio of nanotubes (100–1000), the main body of the tube will remain unaffected. Complex end structures can arise, for instance a conical-shaped sharp tip, due to the way pentagons are distributed near the ends for full closure, each topology leading to a different electronic structure due to the presence of these defects at the tip apex.⁷ These topological changes in the atomic structures near the end of closed carbon nanotubes are known to initiate sharp resonant states in the DOS close to the Fermi energy region,⁸ affecting locally the electronic properties of the system. The strength and the position of these states with respect to the Fermi level depend sensitively on the relative positions of pentagons and their degree of confinement at the tube ends.⁹

Figure 3 illustrates the variations of the density of states along a (10,10) nanotube capped by a hemispherical C_{240} tip apex containing six pentagons in a five-fold symmetric arrangement.⁹ A prominent peak appears just above the Fermi level, which is associated with the presence of the pentagon at the tip apex. In principle, as for all the *armchair* class of nanotubes, this tube is already metallic,

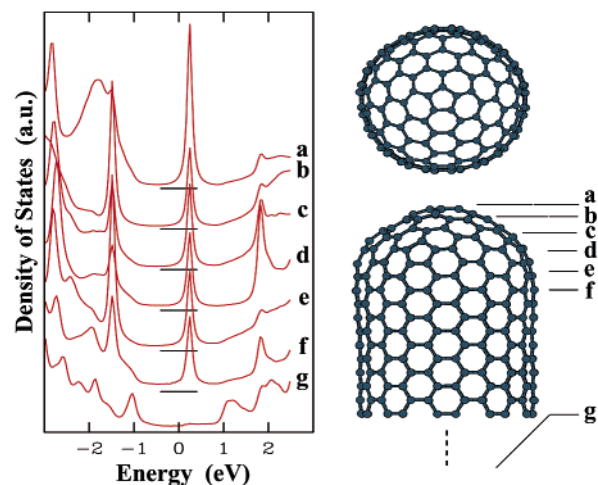


FIGURE 3. Densities of states along a (10,10) nanotube capped with half a C_{240} molecule. The horizontal bars indicate zero densities. The Fermi level is located at zero energy. The DOS curves are averaged over the atoms composing the sections labeled by a–g on the right-hand side.

but there is a huge increase of density of states near the Fermi energy toward the apex. This would imply a corresponding enhancement of the field emission current, and a feature should develop in the energy distribution of field-emitted electrons from an array of such carbon nanotips. Different tip apex topologies lead to peak location in the valence or conduction regions. This indicates that the relative position of pentagons in the tip apex is more important than the global shape (conical or hemispherical) of the cap to determine the position of the localized states.⁸ Increasing the diameter of the tip apex also results in a broadening of the peak, presumably due to a reduced confinement of the pentagons. Detecting these localized states at the tip apex of carbon nanotubes using scanning tunneling spectroscopy⁸ is thus a good way to determine the tip topology, and consequently the symmetry configuration of the tube body. Important physical attributes of nanotube properties that have been seen, such as field emission from nanotube tips⁹ and enhanced oxidation reaction at the tips,¹¹ should be related to the presence of such states.

3. Intramolecular Junctions

Carbon nanotube intramolecular junctions, formed by interposing one or multiple topologic pentagon–heptagon (5/7) defects in the hexagonal structure between two nanotube segments of different helicity (different electronic properties), have also been theoretically proposed long ago for their potential in the creation of nanoelectronic devices.^{12–15} These carbon-based nanostructures could function as molecular-size metal–semiconductor, metal–metal, or semiconductor–semiconductor nanojunctions. Both the existence of such atomic-level structures and the measurement of their respective electronic properties have recently been resolved experimentally.^{16,17} When the pentagon is attached to the heptagon, as in the aniline structure, it creates only topological changes (but no net disclination) which can be treated as a single local

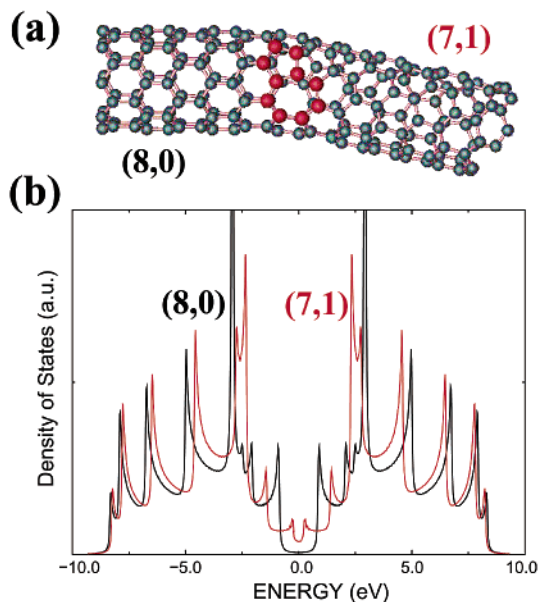


FIGURE 4. (a) Atomic structure of an (8,0)–(7,1) intramolecular carbon junction.¹⁵ The large red balls denote the atoms forming the heptagon–pentagon pair. (b) The electron density of states related to the two perfect (8,0) and (7,1) nanotubes are also illustrated in black and red, respectively.

defect. Such a pair will create only a small local deformation in the width of the nanotube and may also generate a small change in the helicity, depending on its orientation in the hexagonal network. Figure 4 shows the connection, using a single 5/7 pair, between two nanotubes exhibiting different electronic properties. In the tight-binding π -electron approximation, the (8,0) nanotube has a 1.2 eV gap, and the (7,1) tube is a metal (although a small curvature-induced gap is present close to the Fermi¹⁵). Joining a semiconducting nanotube to a metallic one, using a 5/7 pair incorporated in the hexagonal network, can thus be proposed as the basis of a nanodiode (or molecular diode) for nanoelectronics.^{12–15}

4. Carbon Nanotubes under Irradiation

Single-wall carbon nanotubes have also been observed to respond to uniform atom loss through surface reconstruction and drastic dimensional changes.¹⁸ As mentioned in the Introduction, a single-wall carbon nanotube represents the ideal closed surface crystal of monoatomic layer thickness and possesses unique electronic properties due to their small diameters and lattice orientation. The dimensional stability of these structures is thus central to any possible applications of this material in the future. If atoms are continuously extracted at random from their honeycomb lattice, for example through irradiation or during re-evaporation during growth, how will such a surface respond? The result could be either a highly defective structure with the original size or an entirely reconstructed atomic network shrunk in size. Experimental microscopic observations¹⁸ during controlled electron irradiation of isolated single-wall nanotubes clearly evidence drastic shrinkage of these nanosized cylinders, with

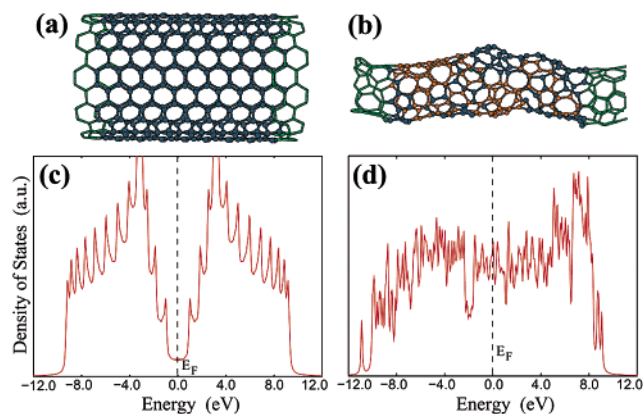


FIGURE 5. Surface reconstruction of (a) a (10,10) single-wall carbon nanotube ($\phi = 1.36$ nm) after a random extraction of 200 carbon atoms along the entire tube surface. Although the reconstructed surface is highly defective (b), the carbon system is still a rough cylinder, the diameter value of which is ~ 0.7 nm, containing 15 5/7 pair defects (in light brown). The corresponding electronic DOS are also illustrated in (c) and (d), respectively.

diameter decreasing from ~ 1.4 nm to incredible values as small as 0.4 nm (the smallest nanotube size ever observed).

Under uniform irradiation conditions, atom removal from the irradiated nanotubes occurs at a slower rate as long as irradiation persists. Atom loss creates vacancies which could further cluster into larger holes in the structure, and due to the dangling bonds associated with these defects, the system will become energetically unstable. By mending these holes through atomic rearrangements, the surface of the original nanotube reconstructs into a highly defective monoatomic layer cylinder of smaller diameter. To understand the nature of surface reconstructions in single-wall nanotubes during atom removal from the surface, molecular dynamics calculations have been performed.¹⁸ The simulation illustrates that the surface reconstruction and size reduction of a perfect (10,10) nanotube (Figure 5a) occur mainly through dangling bond saturation, thus forming nonhexagonal rings and 5/7-like defect pairs in the nanotube lattice. During the course of the simulation, most of the holes, produced by vacancy creation in the lattice, mend as two-coordinate carbon atoms try to recombine, thus forming a mainly three-coordinate, highly defective carbon network. Nonhexagonal rings such as squares, pentagons, heptagons, octagons, nonagons, and decagons were observed at certain stages of the surface reconstruction. However, the unstable high-membered rings are found to disappear by the Stone–Wales mechanism, thus leading the structure to be mainly constituted of five-, six-, and seven-membered rings. Figure 5b presents the reconstructed rough surface of the (10,10) nanotube when half of the atoms in the original model were extracted. Fifteen 5/7-like defect pairs are present in this final topology, leading to an important increase of the DOS close to the Fermi energy. Although the metallic behavior of the reconstructed nanotube is obvious, the van Hove singularities (sharp peaks in the DOS), observed in Figure 5c for a perfect tube, have disappeared in Figure 5d, sug-

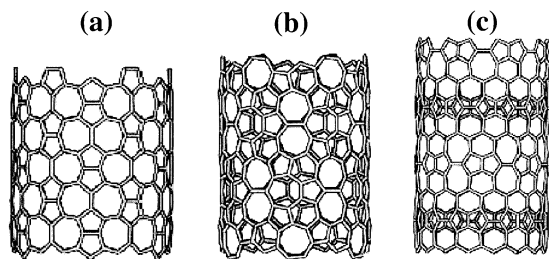


FIGURE 6. Nonchiral Haeckelite nanotubes of similar diameter ($\phi = 1.4$ nm). (a) Nanotube segment containing only heptagons and pentagons paired symmetrically. (b) Nanotube segment exhibiting repetitive units of three agglomerated heptagons, surrounded by alternating pentagons and hexagons. (c) Nanotube segment containing pentalene and heptalene units bound together and surrounded by six-membered rings.

gesting less confinement of the electrons in the radial and circumferential directions of the nanotube and confirming a smaller one-dimensional nature of the conduction within single-wall defective nanotubes.

5. Haeckelite Nanotubes

Following the previous idea of increasing the metallic behavior of the nanotubes, a novel class of perfect crystals, consisting of layered sp^2 -like carbon and containing periodic arrangements of pentagons, heptagons, and hexagons, has been proposed.¹⁹ These sheets are rolled up so as to generate single-wall nanotubes (Figure 6), which resemble locally the radiolaria drawings of Ernst Haeckel.¹⁹ These “ideally” defective tubes exhibit intriguing electronic properties: local density of states (LDOS) calculations of all Haeckelite tubes revealed an intrinsic metallic behavior, independent of orientation, tube diameter, and chirality. Particularly, an unusually high intensity LDOS peak at the Fermi level is noticed for the family of tubes depicted in Figure 6b, thus suggesting the possible existence of superconductivity, as the electron–phonon coupling is expected to be also enhanced by the tube curvature. Our calculations also reveal that these Haeckelite structures are more stable than C_{60} and have energies of the order of 0.3–0.4 eV/atom with respect to graphene, allowing the potential synthesis of this new class of nanotubes.

Considering the universal metallicity properties of Haeckelites, they should offer advantages compared to carbon nanotubes in applications. If they can be manufactured, there is no necessity for diameter or helicity selection to separate metallic structures (i.e., for electronic interconnect applications). But how can one envision making these structures in the laboratory? One could use single-walled nanotubes as templates to generate these architectures. In the previous section, it was shown that electron irradiation results in the lattice reconstructions in single-wall nanotubes, resulting in nanotubes with penta–hexa–hepta rings.¹⁸ Similar experiments using different radiation sources coupled with mechanical compression/stretching (which could also initiate stone-wales transformation) of single-wall nanotubes may also lead to tubules and sheets containing pentagons, heptagons,

and hexagons. An alternative route to Haeckelites could be chemical surface reconstruction processes using strong acids or halogens, which could promote defects saturated with functional groups. Subsequent temperature annealing in inert gases will be necessary to achieve covalently bonded structures containing pentagons, heptagons, and hexagons. However, these synthetic processes would probably not lead to *perfect* and *symmetric* Haeckelite nanotubes, but they will most certainly lead to tubular covalent structures with metallic properties. Identification of these structures, even if they are successfully synthesized, is going to be challenging; scanning tunneling microscopy (STM) could be used to identify their structure and distinguish them from normal carbon nanotubes. But considering that pentagonal and heptagonal defects are not easily identifiable by STM, finding Haeckelites will be quite challenging. Further theoretical STM studies and electron diffraction simulations are necessary for their identification. The Raman effect is also extremely useful for providing information about defects in individual nanotubes; Haeckelite tubes certainly possess a peculiar Raman signature.

6. Coalescence of Carbon Nanotubes

The coalescence of single-wall nanotubes has also been studied in situ in a transmission electron microscope.²⁰ Two of the outer tubes present in a bundle can coalesce under electron irradiation at high temperature, leading to a larger diameter cylinder of nearly double the circumference (4 times the cross section). Intermediate stages of coalescence are also observed in situ (see ref 20). Such processes are frequently observed at the edge of the bundle, probably because free space is needed to establish the merger. It is also hard to observe clearly any coalescence taking place in the interior of the bundles due to nanotube multidirectional overlapping, which reduces image contrast during observation. The merging process is investigated at the atomic level using molecular dynamics simulations.

During the calculation, two adjacent (10,10) nanotubes, containing a few random vacancies and dangling bonds, along the nearest-neighboring edge coalesced into a unique single-wall tube at 1000 °C (Figure 7a–c). The vacancies are found to induce coalescence via a zipper-like mechanism, imposing a continuous reorganization of atoms on individual tube lattices along adjacent tubes. Other topological defects, such as 5/7 pair defects, induce the polymerization of tubes. Coalescence seems to be restricted to tubes with the same chirality, explaining the low frequency occurrence of this event.

7. Welding Carbon Nanotubes

Following the same idea of merging nanostructures, covalently connected crossed single-wall carbon nanotubes have recently been created using electron beam welding at elevated temperatures.²¹ These molecular junctions of various geometries (“X”, “Y”, and “T”) are found to be stable after the irradiation process. To study the

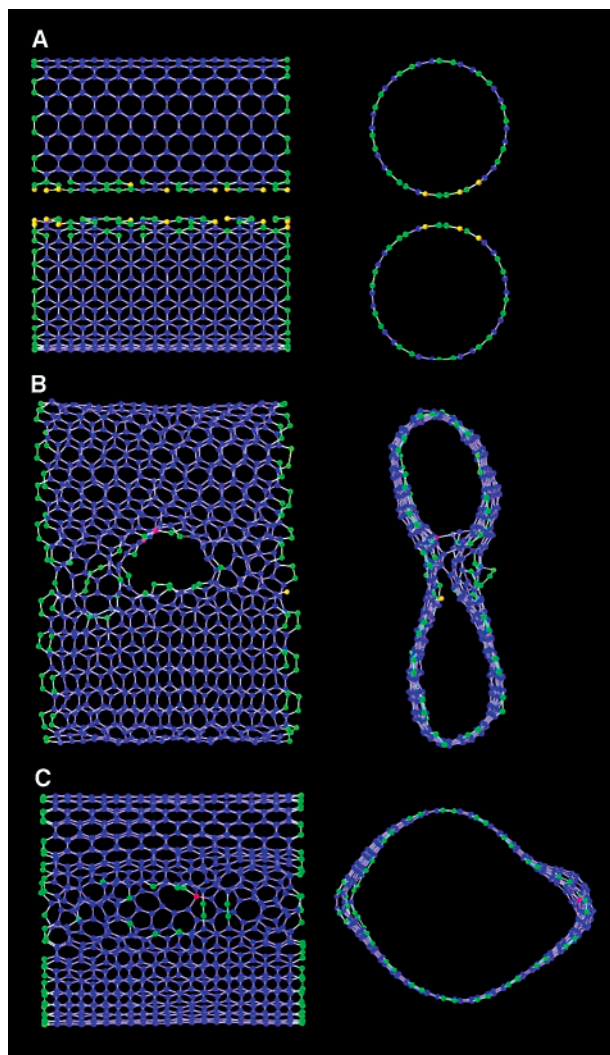


FIGURE 7. Sequences of coalescence (side and sectional views from a–c) between two adjacent (10,10) carbon nanotubes ($\phi = 1.36$ nm) into a unique single-walled tube of larger diameter. The two nanotubes (a) were gradually heated to 1000 °C in order to accelerate the creation of interlinks and the surface reconstruction. After 100 ps, the connection between the two carbon networks has been formed (b), and the “zipping” mechanism is proceeding. After 150 ps, the coalescence is completed (c). The carbon system is now a cylinder with a diameter of about 2.6 nm.

relevance of some of these nanostructures, various models of ideal molecular junctions have been generated. The presence of heptagons is found to play a key role in the topology of nanotube-based molecular junctions.²² Figure 8 depicts an ideal “X” nanotube connection, where a (5,5) armchair nanotube intersects an (11,0) zigzag tube. To create a smooth topology for the molecular junctions, six heptagons have been introduced at each crossing point.

The calculation of the local densities of states has been performed in order to investigate the electronic properties of these molecular junctions. Both the metallic character of the (5,5) nanotube and the semiconducting behavior of the (11,0) nanotube are illustrated in Figure 8b. The LDOS of the regions where the two nanotubes cross reveals an enhancement of the electronic states at the Fermi level, thus suggesting a strong metallic behavior (Figure 8b). These metallic sites (tube intersections) may

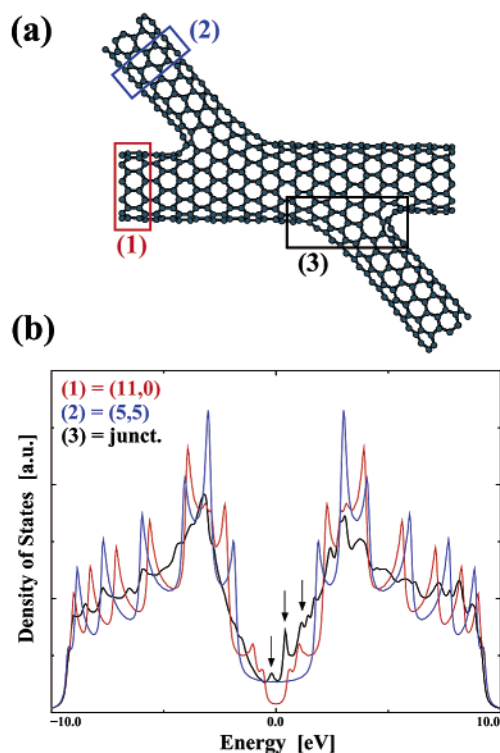


FIGURE 8. Electronic properties of an ideal X-junction (a), created by intersecting a (5,5) tube with an (11,0) tube. (b) One-dimensional electronic densities of states of a semiconducting (11,0) nanotube (red curve), a metallic (5,5) nanotube (blue curve), and averaged over the intersecting region of the molecular junction (black curve). The Fermi level is positioned at zero energy. Localized states due to the presence of defects are indicated by arrows.

well behave as quantum dots when embedded in a semiconducting tubular system. It is also notable that the presence of localized donor states in the conduction band (as indicated by arrows) is caused by the presence of heptagons. The novel small peak on the valence band (also shown by arrow), close to the Fermi energy, can probably be attributed to the high curvature of the graphitic system. The van Hove singularities present in the LDOS of the two achiral nanotubes are drastically less pronounced in the junction region (Figure 8b), thus illustrating a clear loss of the one-dimensional character in this site. Local density of states of junction models, such as those created by irradiation, are described to suggest their importance in electronic device applications. The results are suggested to pave the way toward controlled fabrication of nanotube-based molecular junctions and network architectures exhibiting exciting electronic and mechanical behavior.

8. Doping Carbon Nanotubes

On one hand, boron doping can be carried out by growing tubes in a carbon arc using a BN-rich consumable anode.²³ On the other hand, nitrogen-doped carbon nanotubes can be synthesized by pyrolyzing ferrocene/melamine mixtures at elevated temperatures.²⁴ Changes in the electronic structure of carbon nanotubes due to the introduction of boron and nitrogen in the lattice have been identified using scanning tunneling spectroscopy.^{23,24} Both boron-

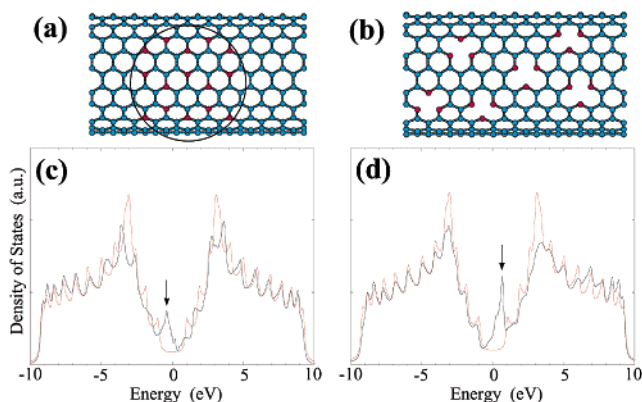


FIGURE 9. Electronic properties of carbon nanotubes doped with (a) boron [B atoms are bonded to three C atoms (B, red spheres; C, blue spheres)] and (b) nitrogen [N atoms are bonded to two C atoms (N, red spheres; C, blue spheres)]. (c) One-dimensional electronic densities of states of a B-doped (10,10) nanotube with a BC_3 island (encircled region) (black curve) compare to an undoped one (red curve). (d) One-dimensional electronic densities of states of a randomly N-doped (10,10) nanotube with pyridine-like defects (black curve) compare to an undoped one (red curve). The Fermi levels are positioned at zero energy. Localized acceptor states (c) and donor states (d) are due to the presence of B and N doping, respectively, and are indicated by arrows.

and nitrogen-doped tubes are metallic with no apparent band gap, in contrast to undoped tubes with varying electronic character. However, in both cases, the LDOS exhibit strongly localized acceptor states (p-doping) or donor states (n-doping) near the Fermi level. First-principles calculations show that changes in the LDOS of boron-doped tubes,²³ as determined from tunneling microscopy, must be interpreted in terms of nanodomains of BC_3 islands (Figure 9a) and not as isolated substitutional species. However, pyridine-like N structures (Figure 9b) are responsible for the metallic behavior and the strong electron donor states observed near the Fermi level in the LDOS of nitrogen-doped tubes.²⁴

The temperature-dependent thermoelectric power of boron- and nitrogen-doped carbon nanotube mats has been measured,²⁵ showing that such dopants can be used to modify the majority carrier conduction from p-type to n-type. These electron (hole)-rich structures are examples of n-type (p-type) nanotubes, which could again pave the way to real molecular heterojunction devices.²⁶

9. Conclusion

Nanotube-based electronics is probably one of the main potential uses of nanotubes. The flexibility of the nanoscale design and the availability of both semiconducting and metallic nanotubes enable a wide variety of configurations. In the present paper, the fascinating electronic properties of carbon nanotubes have been reviewed and tailored by the presence of defects, dopants, etc. Junctions between semiconducting and metallic nanotubes can act as diodes. Junctions between two crossed nanotubes can act as rectifiers. More exotic configurations for nanoscale devices are Y-, T-, or X-junctions.

Although a number of early prototypical nanotube-

based devices have already been made, the production and integration of nanotube components into easily reproducible device structures presents many challenges. Very recently, however, several major steps toward nanotube-based circuitry have been achieved: an array of field-effect transistors has been made by selective burning-off of metallic nanotubes in single-wall nanotube ropes,²⁷ and two groups have assembled field-effect transistors based on single nanotubes into the logic circuits that are building blocks of computers.^{28,29} The realization of single-molecule logic circuits has been a long-standing goal within molecular electronics. A bright new world of nanocircuitry may now be possible, thanks to these recent advances in nanotube electronics.

The author acknowledges Prof. Ph. Lambin, Dr. M. Terrones, Dr. N. Grobert, Dr. E. Hernandez, Dr. H. Terrones, Dr. F. Banhart, and Prof. P. M. Ajayan for their respective collaborations in the different scientific topics mentioned in the present article. J.-C.C. is indebted to the National Fund for Scientific Research (FNRS) of Belgium for financial support. This paper presents research results of the Belgian Program on Interuniversity Attraction Poles (PAI5/1/1) on Quantum Size Effects in Nano-structured Materials, FRFC Project No. 2.4556.99, "Simulations numériques et traitement des données". This work is also carried out within the framework of the EU Human Potential—Research Training Network project under Contract No. HPRN-CT-2000-00128.

References

- (1) Hamada, N.; Sawada, S.; Oshiyama, A. New one-dimensional conductors: graphite microtubules. *Phys. Rev. Lett.* **1992**, *68*, 1579–1581.
- (2) Saito, R.; Fujita, M.; Dresselhaus, G.; Dresselhaus, M. S. Electronic structure of chiral graphene tubules. *Appl. Phys. Lett.* **1992**, *60*, 2204–2206.
- (3) Mintmire, J. W.; Dunlap, B. I.; White, C. T. Are fullerene tubules metallic? *Phys. Rev. Lett.* **1992**, *68*, 631–634.
- (4) Wildoer, J. W. G.; Venema, L. C.; Rinzler, A. G.; Smalley, R. E.; Dekker, C. Electronic structure of carbon nanotubes investigated by scanning tunneling spectroscopy. *Nature* **1998**, *391*, 59–61.
- (5) Odom, T. W.; Huang, J.-L.; Kim, P.; Lieber, C. M. Atomic structure and electronic properties of single-walled carbon nanotubes. *Nature* **1998**, *391*, 62–64.
- (6) Iijima, S.; Ichihashi, T.; Ando, Y. Pentagons, heptagons and negative curvature in graphite microtubule growth. *Nature* **1992**, *356*, 776–778.
- (7) Tamura, T.; Tsukada, M. Electronic states of the cap structure in the carbon nanotube. *Phys. Rev. B* **1995**, *52*, 6015–6026.
- (8) Carroll, D. L.; Redlich, Ph.; Ajayan, P. M.; Charlier, J.-C.; Blase, X.; De Vita, A.; Car, R. Electronic structure and localized states at carbon nanotube tips. *Phys. Rev. Lett.* **1997**, *78*, 2811–2814.
- (9) De Vita, A.; Charlier, J.-C.; Blase, X.; Car, R. Electronic structure at carbon nanotube tips. *Appl. Phys. A* **1999**, *68*, 283–286.
- (10) De Heer, W. A.; Chatelain, A.; Ugarte, D. A carbon nanotube field-emission electron source. *Science* **1995**, *270*, 1179–1180.
- (11) Ajayan, P. M.; Ebbesen, T. W.; Ichihashi, T.; Iijima, S.; Tanigaki, K.; Hiura, H. Opening carbon nanotubes with oxygen and implications for filling. *Nature* **1993**, *362*, 522–525.
- (12) Lambin, P.; Fonseca, A.; Vigneron, J. P.; Nagy, J. B.; Lucas, A. A. Structural and electronic properties of bent carbon nanotubes. *Chem. Phys. Lett.* **1995**, *245*, 85–89.
- (13) Saito, R.; Dresselhaus, M. S.; Dresselhaus, G. Tunneling conductance of connected carbon nanotubes. *Phys. Rev. B* **1996**, *53*, 2044–2049.
- (14) Charlier, J.-C.; Ebbesen, T. W.; Lambin, Ph. Structural and electronic properties of pentagon–heptagon pair defects in carbon nanotubes. *Phys. Rev. B* **1996**, *53*, 11108–11113.
- (15) Chico, L.; Crespi, V. H.; Benedict, L. X.; Louie, S. G.; Cohen, M. L. Pure carbon nanoscale devices: nanotube heterojunctions. *Phys. Rev. Lett.* **1996**, *76*, 971–974.
- (16) Yao, Z.; Postma, H. W. Ch.; Balents, L.; Dekker, C. Carbon nanotube intramolecular junctions. *Nature* **1999**, *402*, 273–276.

- (17) Ouyang, M.; Huang, J.-L.; Cheung, C. L.; Lieber, C. M. Atomically resolved single-walled carbon nanotube intramolecular junctions. *Science* **2001**, *291*, 97–100.
- (18) Ajayan, P. M.; Ravikumar, V.; Charlier, J.-C. Surface reconstructions and dimensional changes in single-walled carbon nanotubes. *Phys. Rev. Lett.* **1998**, *81*, 1437–1440.
- (19) Terrones, H.; Terrones, M.; Hernandez, E.; Grobert, N.; Charlier, J.-C.; Ajayan, P. M. New metallic allotropes of planar and tubular carbon. *Phys. Rev. Lett.* **2000**, *84*, 1716–1719.
- (20) Terrones, M.; Terrones, H.; Banhart, F.; Charlier, J.-C.; Ajayan, P. M. Coalescence of single-walled carbon nanotubes. *Science* **2000**, *288*, 1226–1229.
- (21) Terrones, M.; Banhart, F.; Grobert, N.; Charlier, J.-C.; Terrones, H.; Ajayan, P. M. *Phys. Rev. Lett.*, in press.
- (22) Menon, M.; Srivastava, D. Carbon nanotube T junctions: nanoscale metal-semiconductor-metal devices. *Phys. Rev. Lett.* **1997**, *79*, 4453–4456.
- (23) Carroll, D. L.; Redlich, Ph.; Blase, X.; Charlier, J.-C.; Curran, S.; Ajayan, P. M.; Roth, S.; Rühle, M. Effects of nanodomain formation on the electronic structure of doped carbon nanotubes. *Phys. Rev. Lett.* **1998**, *81*, 2332–2335.
- (24) Czerw, R.; Terrones, M.; Charlier, J.-C.; Blase, X.; Foley, B.; Kamalakaran, R.; Grobert, N.; Terrones, H.; Ajayan, P. M.; Blau, W.; Tekleab, D.; Rühle, M.; Carroll, D. L. Identification of electron donor states in N-doped carbon nanotubes. *Nano Lett.* **2001**, *1*, 457–460.
- (25) Choi, Y.-M.; Lee, D.-S.; Czerw, R.; Chiu, P.-W.; Grobert, N.; Terrones, M.; Reyes-Reyes, M.; Terrones, H.; Charlier, J.-C.; Ajayan, P. M.; Roth, S.; Carroll, D. L.; Park, Y.-W. Submitted.
- (26) Choi, H. J.; Ihm, J.; Louie, S. G.; Cohen, M. L. Defects, quasibound states, and quantum conductance in metallic carbon nanotubes. *Phys. Rev. Lett.* **2000**, *84*, 2917–2920.
- (27) Derycke, V.; Martel, R.; Appenzeller, J.; Avouris, Ph. Carbon nanotube inter- and intramolecular logic gates. *Nano Lett.* **2001**, *1*, 453–456.
- (28) Huang, Y.; Duan, X.; Cui, Y.; Lauhon, L. J.; Kim, K. H.; Lieber, C. M. Logic gates and computation from assembled nanowire building blocks. *Science* **2001**, *294*, 1313–1317.
- (29) Bachtold, A.; Hadley, P.; Nakanishi, T.; Dekker, C. Logic circuits with carbon nanotube transistors. *Science* **2001**, *294*, 1317–1320.

AR010166K